Picosecond time scale modification of forward scattered light induced by absorption inside particles

Myriam Kervella,[1] Françoix-Xavier d'Abzac[1], François Hache[2] Laurent Hespel,[1] and Thibault Dartigalongue[1,*]

[1]*Departement of theorical and applied optics, ONERA, 2 avenue Edouard Belin, BP 74025, 31055 Toulouse cedex, France*

[2]*Laboratory for optics and biosciences, Ecole Polytechnique, 91128 Palaiseau cedex France*

[*]*Thibault.Dartigalongue@onera.fr*

Abstract: The aim of this work is to evaluate the influence of absorption processes on the Time Of Flight (TOF) of the light scattered out of a thick medium in the forward direction. We use a Monte-Carlo simulation with temporal phase function and Debye modes. The main result of our study is that absorption inside the particle induces a decrease of the TOF on a picosecond time scale, measurable with a femtosecond laser apparatus. This decrease, which exhibits a neat sensitivity to the absorption coefficient of particles, could provide an efficient way to measure this absorption.

OCIS codes: (320.7120) Ultrafast phenomena; (290.5850) Scattering, particles; (290.7050) Turbid media; (290.4210) Multiple scattering.

References and links

1. C. F. Bohren and D. R. Huffman, *Absorption and Scattering of Light by Small Particles* (Wiley Interscience, 1983).
2. M. I. Mishchenko, L. D. Travis, and A. A. Lacis, *Scattering, Absorption, and Emission of Light by Small Particles* (Cambridge University Press, 2002).
3. C. Calba, L. Méès, C. Rozé, and T. Girasole, "Ultrashort pulse propagation through a strongly scattering medium: simulation and experiments," J. Opt. Soc. Am. A **25**(7), 1541–1550 (2008).
4. M. Barthélémy, N. Rivière, L. Hespel, and T. Dartigalongue, "Pump probe experiment for high scattering media diagnostics," in *SPIE Optics and Photonics*; San Diego, CA, USA, 2008; Conference Proceedings; Vol. 7065.
5. A. M. Pena, T. Boulesteix, T. Dartigalongue, and M. C. Schanne-Klein, "Chiroptical effects in the second harmonic signal of collagens I and IV," J. Am. Chem. Soc. **127**(29), 10314–10322 (2005).
6. D. Débarre, W. Supatto, A. M. Pena, A. Fabre, T. Tordjmann, L. Combettes, M. C. Schanne-Klein, and E. Beaurepaire, "Imaging lipid bodies in cells and tissues using third-harmonic generation microscopy," Nat. Methods **3**(1), 47–53 (2006).
7. S. A. Malinovskaya and V. S. Malinovsky, "Chirped-pulse adiabatic control in coherent anti-Stokes Raman scattering for imaging of biological structure and dynamics," Opt. Lett. **32**(6), 707–709 (2007).
8. L. Wang, P. P. Ho, C. Liu, G. Zhang, and R. R. Alfano, "Ballistic 2-d imaging through scattering walls using an ultrafast optical Kerr gate," Science **253**(5021), 769–771 (1991).
9. T. Gustavsson, A. Sharonov, and D. Markovitsi, "Thymine, thymidine and thimidine 5′-monophosphate studied by femtosecond fluorescence upconversion spectroscopy," Chem. Phys. Lett. **351**(3-4), 195–200 (2002).
10. W. Tan, Y. Yang, J. Si, J. Tong, W. Yi, F. Chen, and X. Hou, "Shape measurement of objects using an ultrafast optical Kerr gate of bismuth glass," J. Appl. Phys. **107**(4), 043104 (2010).
11. D. Sedarsky, E. Berrocal, and M. Linne, "Quantitative image contrast enhancement in time-gated transillumination of scattering media," Opt. Express **19**(3), 1866–1883 (2011).
12. L. Wang, X. Liang, P. A. Galland, P. P. Ho, and R. R. Alfano, "Detection of objects hidden in highly scattering media using time-gated imaging methods," in Optical Sensing, Imaging, and Manipulation for Biological and Biomedical Applications, Conference SPIE Proceeding, Vol. 4082 (2000).
13. M. Barthélémy, L. Hespel, N. Rivière, B. Chatel, and T. Dartigalongue, "Pump probe experiment for optical diagnosis of very thick scattering media," Aerospace Lab J. **1**, 155–200 (2009).
14. K. M. Yoo, G. C. Tang, and R. R. Alfano, "Coherent backscattering of light from biological tissues," Appl. Opt. **29**(22), 3237–3239 (1990).
15. C. Das, A. Trivedi, K. Mitra, and T. Vo-Dinh, "Short pulse laser propagation through tissues for biomedical imaging," J. Phys. D Appl. Phys. **36**(14), 1714–1721 (2003).

#154880 - $15.00 USD Received 16 Sep 2011; revised 28 Oct 2011; accepted 28 Oct 2011; published 20 Dec 2011

16. C. J. Lee, P. J. van der Slot, and K. J. Boller, "Using ultra-short pulses to determine particle size and density distributions," Opt. Express **15**(19), 12483–12497 (2007).
17. W. Long and D. Burns, "Particle sizing and optical constant measurement in granular samples using statistical descriptors of photon time-of-flight distributions," Anal. Chim. Acta **434**(1), 113–123 (2001).
18. C. Gributs and D. Burns, "Multiresolution analysis for quantification of optical properties in scattering media using pulsed photon time-of-flight measurements," Anal. Chim. Acta **490**(1-2), 185–195 (2003).
19. L. Méès, G. Gréhan, and G. Gouesbet, "Time-resolved scattering diagram for a sphere illuminated by plane wave and focused short pulses," Opt. Commun. **194**(1-3), 59–65 (2001).
20. A. E. Hovenac and J. A. Lock, "Assessing the contributions of surface waves and complex rays to far-field Mie scattering by use of the Debye series," J. Opt. Soc. Am. A **9**(5), 781–795 (1992).
21. N. Rivière, M. Barthélémy, T. Dartigalongue, and L. Hespel, "Modeling of femtosecond pulse propagation through dense scattering media," Proc. SPIE **7065**, 70650X, 70650X-9 (2008).
22. Q. Fu and W. Sun, "Mie theory for light scattering by a spherical particle in an absorbing medium," Appl. Opt. **40**(9), 1354–1361 (2001).
23. J. Shen and H. Wang, "Calculation of Debye series expansion of light scattering," Appl. Opt. **49**(13), 2422–2428 (2010).
24. X. Wang, L. V. Wang, C.-W. Sun, and C.-C. Yang, "Polarized light propagation through scattering media: time-resolved Monte Carlo simulations and experiments," J. Biomed. Opt. **8**(4), 608–617 (2003).
25. S. Avrillier, E. Tinet, and J. M. Tualle, "Fast semianalytical monte carlo simulation for time resolved light propagation in turbid media," J. Opt. Soc. Am. A **9**, 1903–1915 (1996).
26. C. Calba, C. Rozé, T. Girasole, and L. Méès, "Monte Carlo simulation of the interaction between an ultra short pulse and a strongly scattering medium: the case of large particles," Opt. Commun. **265**(2), 373–382 (2006).
27. F. Onofri, "Critical angle refractometry for simultaneous measurement of particles in flow: size and relative refractive index," Part. Part. Syst. Charact. **16**(3), 119–127 (1999).

1. Introduction

The understanding of interactions between light and scattering dense media such as clouds, paints or biological tissues is a major issue as far as optical diagnosis is concerned. In order to carry out such investigation, model systems made up of spherical particles in suspension in a host medium have been widely studied [1, 2]. Femtosecond lasers are bright enough to go through very thick media with tunable wavelength [3, 4], and are used in a wide variety of optical diagnosis and imaging techniques (SHG [5], THG [6], CARS [7], …). Furthermore, thanks to Optical Kerr Gate (OKG) measurements [8] or up-conversion technique [9], it is possible to temporally sample the light going out of the sample with a resolution of approximately 100 *fs* [10] (*i.e.* less than 20 microns spatially). Such experiments are used to isolate ballistic and scattered light (ballistic imaging [11, 12], optical density measurement [13]) or to study the temporal scattering process itself in order to get information about the sample [14–16].

The aim of this work is to evaluate the Time Of Flight (TOF) of light going through a scattering medium on a femtosecond time scale when the particles are absorbing. The influence of absorption processes has been widely studied on longer time scale (nanosecond) and backscattered direction [17, 18]. This will not be the goal of our study as we only focus on the forward direction (few 10^{-4} *Sr* around the laser beam). We will demonstrate that absorption inside the particle induces a decrease of the TOF on a picosecond time scale. This effect appears to be very sensitive to the imaginary part of the particle refractive index.

The influence of absorption inside the particles is not straightforward as it profoundly affects all the microscopic properties of particles: albedo, phase function, absorption and scattering cross sections. We will present a complete numerical scheme in order to evaluate the TOF of light scattered out of a system made up of absorbing particles in the forward direction. We will fully describe how absorption modifies the temporal phase function, the weight of Debye modes, the asymmetry factor, and the albedo. We will show that all these effects should contribute to a global decrease of the TOF on a picosecond time scale. We will then carry out a Monte-Carlo simulation to evaluate the order of magnitude of this effect. We will compare the case of large particles (50 μm radii), exhibiting a neat temporal separation of the Debye mode, with the case of small particles (5 μm radii).

#154880 - $15.00 USD Received 16 Sep 2011; revised 28 Oct 2011; accepted 28 Oct 2011; published 20 Dec 2011

2. Temporal phase function

The first step consists in determining the temporal phase functions, *i.e.*, the probability for a photon to be scattered out of the particle with a given angle θ, and a given delay t. The scattering angle θ is the angle between the incident and scattered vectors (0° corresponds to the forward scattering direction). The time delay t corresponds to the time difference between the outgoing scattered beam and a reference beam propagating through the centre of the particle where the particle has been replaced by the host medium. For our entire study, we consider ultra short laser pulses (*FWHM*=100 *fs*) impinging on spherical particles (refractive index n_{pa}=1.5) in suspension in a host medium (n_{hm}=1.33). This short laser pulse has a spectral bandwidth centred at λ=0.8 μm. For every frequency ω of the laser pulse, we calculate the Jones coefficients S_1 and S_2 thanks to Mie decomposition:

$$\begin{aligned} S_1(\omega,\theta) &= \sum_n \frac{2n+1}{n(n+1)}(\tau_n^1(\theta)a_n(\omega,\theta) - \tau_n^2(\theta)b_n(\omega,\theta)) \\ S_2(\omega,\theta) &= \sum_n \frac{2n+1}{n(n+1)}(\tau_n^2(\theta)a_n(\omega,\theta) - \tau_n^1(\theta)b_n(\omega,\theta)) \end{aligned} \quad (1)$$

where τ_n^1 and τ_n^2 are the angle-dependent functions and a_n and b_n are the Mie scattering coefficients and can be found in [1]. The angular phase function $P(\omega,\theta)$ is directly proportional to $|S_1(\omega,\theta)|^2+|S_2(\omega,\theta)|^2$. The temporal and angular phase function $P(t,\theta)$ is obtained by Fourier transformation of $P(\omega,\theta)$ [19] and is represented in Fig. 1(a). Different modes can be observed for different angles and time delays. In order to understand this behaviour, we introduce Debye modes [20]: a_n (and b_n) can be rewritten as followed:

$$a_n^p = \frac{1}{2}(1 - R_{n,a}^{hm} - \sum_{p=1}^{\infty} T_{n,a}^{hm}(R_{n,a}^{pa})^{p-1}T_{n,a}^{pa}) \quad (2)$$

where p denotes the order of the Debye mode. T and R denote transmission and reflection coefficients through the interface particle/host medium which can be found in [20]. The indices a and n ($R_{n,a}$, $T_{n,a}$) refer to the coefficient a_n and an equivalent formula can be written for b_n. By using decomposition (2) in Eq. (1), it is now possible to calculate the partial phase function of the different modes. A schematic representation [21] of Debye mode can be found on Fig. 2. Note that all phase functions are normalized to the corresponding non temporal phase function. The mode 0 (Fig. 1(b)) is mainly directed in the forward direction with 0 delay. It is a surface mode propagating along the interface host medium/particle. A very small part of the energy shows up for greater angle at negative delay, (*i.e.* before the "zero" reference beam) as it corresponds to light reflected at the front interface. The mode 1 (Fig. 1(c)) mainly corresponds to a transmission of energy through the bulk of the particle. It is approximately delayed of $\Delta t = (n_{pa}-n_{hm})*(2R/c)$, compared to the mode 0, where R is the radius of the particle, c the speed of light in vacuum, n_{pa}, and n_{hm} denote the refractive index of the particle and of the host medium respectively. Mode 2 (Fig. 1(d)) undergoes 1 internal reflection and is responsible of the rainbow effect. Mode n undergoes $n-1$ internal reflections. One of the key points of our study is to evaluate how absorption modifies the temporal phase function and this will be done in the next section.

#154880 - $15.00 USD Received 16 Sep 2011; revised 28 Oct 2011; accepted 28 Oct 2011; published 20 Dec 2011

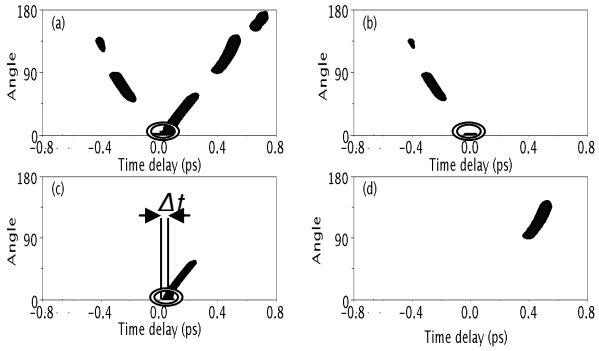

Fig. 1. 2D plot of normalized temporal phase functions P(t,θ) ((a) total, (b) for mode 0, (c) for mode 1 and (d) for mode 2) for a 50 µm particle radius. More than 80% of energy is contained inside the rings, i.e. in the forward direction. The mode 1 is delayed by Δt compared with the mode 0.

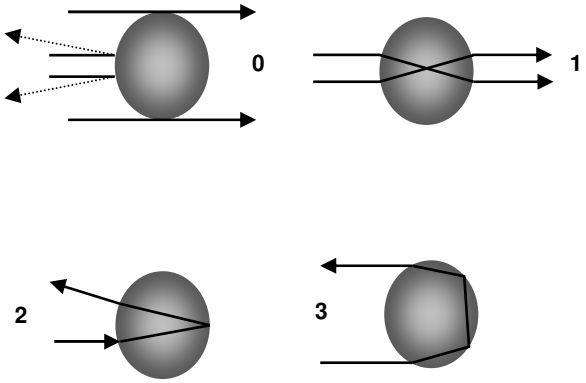

Fig. 2. Schematic representation of the first four Debye modes. Mode 0 is a surface reflection mode at the interface of the particle. Mode 1 is a transmission mode through the bulk of the particle. For information, we also show the second and the third modes which undergo respectively one and two internal reflections.

3. Debye mode weight

We have carried out calculation of temporal phase functions of the different Debye modes for a significant and arbitrary imaginary part of the refractive index of the particle, k_{pa}. The two key results of our study are the following. First, we have compared different temporal profiles $P_\theta\ (t)$ with and without absorption. No significant change can be observed. However, k_{pa} profoundly affects the relative weight of the Debye modes. To show this second result, we have calculated the energy I_p scattered for the modes p:

$$I_p = \frac{2\pi}{|k|^2}\sum_{n=1}^{\infty}(2n+1)\left(\left|a_n^p\right|^2+\left|b_n^p\right|^2\right) \tag{3}$$

where k is the wave number. We have calculated the weight of the different modes on a large domain of particle size. As soon as the radii are bigger than 1 μm, all the energy is scattered either in mode 0 or 1. We represent (Fig. 3) the ratio I_1/I_0. When $k_{pa} = 0$, the energy is almost equally shared between mode 0 and mode 1, I_1/I_0 is very close to 1. When k_{pa} increased, the weight of mode 1 strongly decreases as it corresponds to a mode going through the absorbing

#154880 - $15.00 USD Received 16 Sep 2011; revised 28 Oct 2011; accepted 28 Oct 2011; published 20 Dec 2011

bulk of the particle. Only mode 0 remains as it propagates at the interface. This effect is more important for large particles as the energy loss inside the particle is larger.

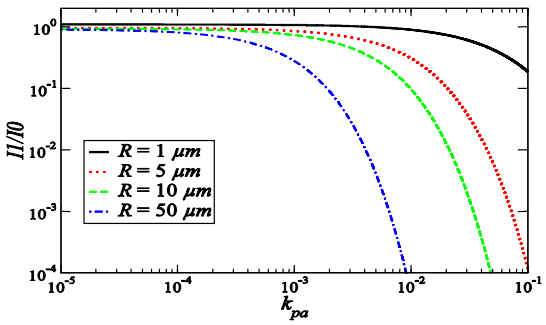

Fig. 3. Ratio I_1/I_0 between the weight of the mode 0 and the mode 1 (Eq. (3)) as a function of k_{pa} for different particle radii.

For non absorbing particles, 50% of the energy goes through mode 1 and is delayed of $\Delta t = (n_{pa}-n_{hm})*(2R/c)$. For absorbing particles, 100% of the energy should be scattered through mode 0 and not be delayed. As a result, the global TOF should decrease when k_{pa} increases. In addition to the scattering process itself, we have to consider the TOF between two scattering events. When the phase function is mainly directed in the forward direction, the trajectory of light is very straight, and the TOF is very small. As the contrary, when the phase function is isotropic, the trajectory of the light is more complex, and the global time of flight is longer. As a result, we need to understand the dependence between the angular distribution and k_{pa}.

4. Asymmetry factor

The angular dependence is modified when k_{pa} strongly increases [22]. We introduce the asymmetry factor g defined and calculated as followed [1]:

$$g = \frac{1}{2}\int_0^{\pi} P(\cos\theta)\sin\theta\cos\theta d\theta$$

$$g = \frac{2\sum_{n=1}^{\infty}\frac{n(n+2)}{n+1}\mathrm{Re}(a_n a_{n+1}^{*} + b_n b_{n+1}^{*}) + \frac{2n+1}{n(n+1)}\mathrm{Re}(a_n b_n^{*})}{\sum_{n=1}^{\infty}(2n+1)(|a_n|^2 + |b_n|^2)} \tag{4}$$

This factor g gives information about the sharpness of the phase function (*i.e.*, g very close to 1 for sharp phase function and close to 0 for isotropic phase function). By using decomposition (2) in this formula, we are able to calculate the asymmetry factor of the total and partial phase functions. The results are represented (Fig. 4) for increasing value of k_{pa}. For mode 0, g is a constant and almost equal to 1. The phase function of mode 0 is very sharp and peaked in the forward direction and the absorption of the bulk does not modify this surface mode. On the opposite, mode 1 is more isotropic than mode 0. The total phase function becomes more and more peaked in the forward direction when k_{pa} increases (complete overlap with mode 0 for great value of k_{pa} as observed in [23]).

#154880 - $15.00 USD Received 16 Sep 2011; revised 28 Oct 2011; accepted 28 Oct 2011; published 20 Dec 2011

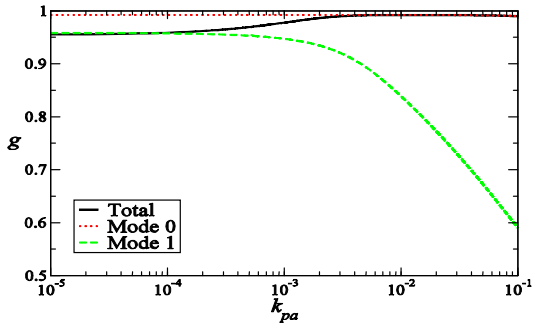

Fig. 4. Total asymmetry factor (solid black line), asymmetry factors of mode 0 (dotted red line) and mode 1 (dotted green line) as a function of k_{pa} for a 50µm particle radius (Eq. (4)).

The TOF should decrease even more when k_{pa} increases as the angular distribution of the scattered light is sharper for mode 0 compared to mode 1. The trajectory of light through the medium will be straighter. The time of flight decreases because the asymmetry factor increases (straighter trajectory), and because mode 1 is killed (no more Δt at the crossing of the particle). In the following section, we show that the decrease of TOF can be also due to the modification of the scattering/absorbing cross section.

5. Scattering and absorption cross sections

One needs to evaluate the influence of k_{pa} over the different cross sections: scattering σ_{sca}, absorption σ_{abs}, and extinction σ_{ext}. Partial extinction cross-section σ_{ext}^{p} verifies the following formula:

$$\sigma_{ext}^{p} = \frac{2\pi}{k^2}\sum_{n=1}^{\infty}(2n+1)\,\mathrm{Re}\left\{a_n^p + b_n^p\right\} \tag{5}$$

where a_n^p and b_n^p can be found in the Eq. (2). We have also carried out similar calculations for σ_{ext}^{mie} using regular expressions for a_n and b_n based on Mie theory, still valid for absorbing particles [1]. We define the different extinction efficiencies q_{ext}^{p}:

$$q_{ext}^{p} = \sigma_{ext}^{p} \big/ (\pi R^2) \tag{6}$$

q_{ext}^{mie} denotes the efficiency obtained with the regular Mie theory. We represent (Fig. 5) the evolution of three different extinction efficiencies (q_{ext}^{0}, $q_{ext}^{0} + q_{ext}^{1}$ and q_{ext}^{mie}) for increasing radii. Without absorption, one can observe 3 regimes: (i) the increase of q_{ext}^{mie} with R for small particles corresponds to the Rayleigh regime, (ii) oscillations of q_{ext}^{mie} with R belong to the Mie regime and (iii) q_{ext}^{mie} is very close to 2 for large particles in the so-called non selective regime. The agreement between $q_{ext}^{0} + q_{ext}^{1}$ and q_{ext}^{mie} is very good except for Rayleigh regime where more than 2 Debye modes are needed to describe the scattering process. For increasing value of k_{pa}, mode 1 is killed. The q_{ext} curve overlaps the one obtained for mode 0 only, and oscillations disappear. The consequence is a slight increase or decrease of q_{ext}^{mie} when k_{pa} increases, depending on the particle radius. This is the well known process called absorption edge [1].

#154880 - $15.00 USD Received 16 Sep 2011; revised 28 Oct 2011; accepted 28 Oct 2011; published 20 Dec 2011

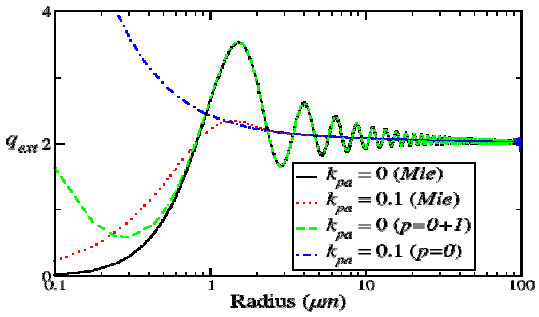

Fig. 5. Extinction efficiency q_{ext} (Eq. (6)) as a function of the particle radius. Total (solid black and dotted red lines) and partial (dotted green and blue lines) extinction efficiencies are plotted for different values of k_{pa}.

We now evaluate the impact of k_{pa} over the scattering and absorbing cross sections when we calculate the albedo Ω:

$$\Omega = \sigma_{sca}^{mie} \Big/ \sigma_{ext}^{mie} \tag{7}$$

When there is no absorption, all the energy is scattered: $\sigma_{sca}^{mie} = \sigma_{ext}^{mie}$ (Ω = 1). When k_{pa} increases, σ_{ext}^{mie} is not modified (if we neglect the absorption edge effect described above). Half of the total energy that should have been scattered in mode 1 is now absorbed inside the particle. As a result, we expect that $\sigma_{abs}^{mie} = \sigma_{sca}^{mie} \approx \sigma_{ext}^{mie} / 2$. Indeed, when k_{pa} increases, the albedo decreases from 1 to 0,5 (Fig. 6). The main consequence for the time of flight is that single scattering trajectory will have a more important weight compared to multiple scattering trajectory, as there are energy losses after every scattering event. The energy decay is roughly equal to 2^{-m} where m is the number of the scattering events. One can note that single scattering trajectory corresponds to a shorter pathway, and shows up for earlier delay than multiple scattering one. Hence, the absorption inside the particle induces a decrease of the global TOF of the light.

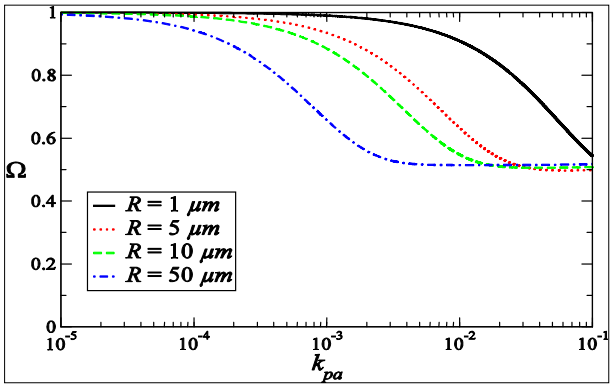

Fig. 6. albedo Ω (Eq. (7)) as a function of k_{pa} for different particle radii.

6. Monte Carlo scheme

In order to evaluate the TOF decrease, we developed a Monte Carlo simulation scheme. A great part of random tests is explained in [21]: this complex process is simulated by a

#154880 - $15.00 USD Received 16 Sep 2011; revised 28 Oct 2011; accepted 28 Oct 2011; published 20 Dec 2011

succession of elementary events (scattering, absorption by the particle). In order to simplify our study, we consider a medium without interfaces. We have carefully compared our simulation code with published result in the case of non absorbing particle [3,24]. In order to obtain the best signal to noise ratio, we use a semi-analytical Monte Carlo approach [25] for small particles, and a full Monte Carlo for large particles [26]. We have carefully checked the agreement of these two approaches for a great variety of radii. We consider a small detector in the forward direction. The solid angle is equal to 5.10^{-4} *Sr*. We consider an optical path of 1 cm, and an Optical Thickness *O.T.* = 20. We verified that *O.T.* is not significantly modified for the value of k_{pa} we considered.

In Fig. 7, we report the relative scattered intensity as a function of time delay for particles of 5 μm. For k_{pa} = 0.001, we observe a global decrease of the intensity, and a small but yet measurable decrease of TOF (few picoseconds can be detected with a streak camera [14] or femtosecond laser experiment [11]). For stronger value (k_{pa} = 0.01), the reduction of TOF is more visible. The scattered light tends to overlap the ballistic light (ballistic distribution is centred on zero-delay and has 100 *fs* line width (FWHM)).

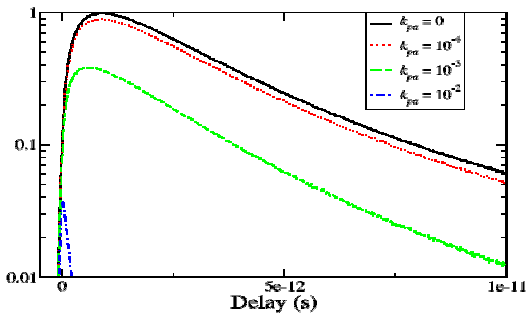

Fig. 7. Relative scattered intensity as a function of TOF for different values of k_{pa} and for a 5 µm particle radius.

Within the same conditions as above, we now study larger particles (R = 50 μm). With no absorption, two separated lobes can be observed (Fig. 8). In order to understand the physical origin of these two lobes, we represent (Fig. 9) the partial TOF curve, as we have kept track of the amount of mode 0 and mode 1 scattering events in our modelling scheme. The first lobe corresponds to pathways with only "0 mode" scattering events. A single "mode 1 scattering" event in the pathway greatly reduces the efficiency of collection. This is due to the asymmetry factor of mode 1 that spreads the angular distribution of the scattered light. As we only detect energy in the forward direction with a small solid angle, the collection efficiency dramatically decreases. The high efficiency of collection in "pure mode 0 pathway" completely balances its very poor probability of occurrence. As a result, a very neat temporal separation between the 2 lobes can be observed. Indeed, the delay shift observed between pure 0 scattering pathway and single mode 1 event scattering pathway is roughly equal to Δt. The "0 lobe", also called "snake-like photon", completely overlaps the ballistic contribution (not represented here as it is thousand times smaller compared to the "snake-like contribution"). A slight increase of the absorption (k_{pa} = 10^{-5}) induces a detectable change in the temporal distribution: we can observe a neat decrease of the delayed lobe. Here again, for high values of k_{pa}, only the mode 0 remains whereas higher modes are absorbed.

#154880 - $15.00 USD Received 16 Sep 2011; revised 28 Oct 2011; accepted 28 Oct 2011; published 20 Dec 2011

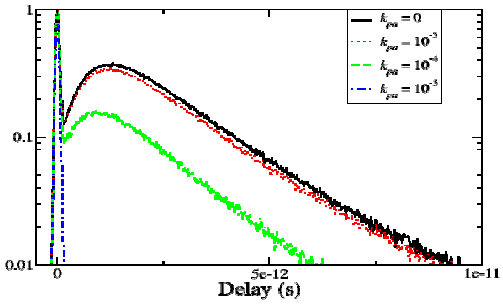

Fig. 8. Relative scattered intensity as a function of TOF for different values of k_{pa}, and for a 50 µm particle radius.

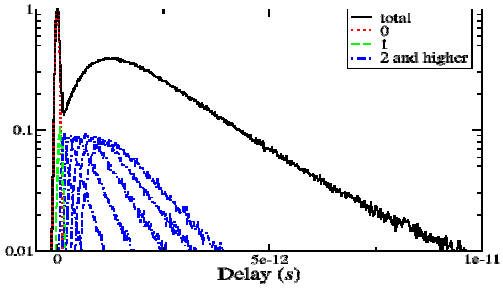

Fig. 9. Relative scattered intensity as a function of TOF for different amount of mode 1's event when $k_{pa} = 0$ and for a 50 µm particle radius.

7. Discussion

We want to evaluate independently the influence of the 3 phenomena (albedo, Debye mode weight and asymmetry factor). Though, it is not possible to dissociate the angular and temporal dependence of the phase function. As a result, we have studied 2 cases. Case a/ k_{pa} modifies the angular and temporal distribution (sections 3&4), but we consider that there is no energy loss during the scattering process. Case b/ the photon can be lost during the scattering process (section 5), but we keep the temporal phase function as if the particles were non absorbing. We report (Table 1) the corresponding average delay τ, τ_a and τ_b.

Table 1. Results of the simulation. Index *a* and *b* denotes respectively the influence of albedo and phase function.

R	k_{pa}	*O.T.*	*g*	*Ω*	τ *(ps)*		
5 µm	0	20	0.906	1	3.7		
	10^{-4}	20.02	0.907	0.99	3.6		
	10^{-3}	20.21	0.913	0.93	τ =2.9	τ_a=3.5	τ_b=3.1
	10^{-2}	21.45	0.954	0.63	0.4		
50 µm	0	20	0.955	1	2.54		
	10^{-5}	20.01	0.956	0.99	2.47		
	10^{-4}	20.03	0.959	0.94	τ =1.83	τ_a=2.27	τ_b=2.1
	10^{-3}	20.18	0.978	0.65	7.10^{-3}		

#154880 - $15.00 USD Received 16 Sep 2011; revised 28 Oct 2011; accepted 28 Oct 2011; published 20 Dec 2011

For small and large particles, both effects (albedo and phase function) induce a decrease of τ. While considering the two processes, the effect is even stronger. For small particles (Fig. 7), the average intensity of scattered light decreases a lot with k_{pa}. This effect could be tracked thanks to a non-temporal measurement which is more straightforward. Nevertheless, the TOF is an absolute measurement, less sensitive to the fluctuation of the intensity of the laser or other experimental noise. This could be relevant to measure k_{pa} bigger than 10^{-3}. For large particles, a measurement of TOF is even more sensitive as the snake like peak remains unchanged and can be used as a reference: it precisely defines the 0 delay, and it allows a measurement of the ratio of intensity of the 2 lobes. We have checked that the slight attenuation of the snake like peak when $k_{pa} = 10^{-3}$ is only induced by the increase of *O.T.* from 20 to 20.18 (absorption edge). When $k_{pa} = 10^{-5}$, absorption is not detectable with classical technique, there is no variation of the optical thickness or modification of the phase function (Table 1).

In order to evaluate the impact of the real part of the refractive index n_{pa} compared to k_{pa}, we have considered a variation of these two parameters of the same magnitude ($\Delta n_{pa} = \Delta k_{pa} = 10^{-5}$) and calculated the impact on the average time of flight τ. For particle of 50 μm, the impact of k_{pa} is 40 times bigger than the impact of n_{pa} (20 times for particle of 5 μm). This method could be coupled with other methods more sensitive to n_{pa} such as refractometry or rainbow [27] and might be a powerful tool to measure the absorption coefficient of particle. This could be very useful to evaluate the water content of particle, the concentration of absorbing molecule at the surface of a particle or the temperature of a water droplet.

The phenomenon we have simulated is observed on a picosecond time scale and could not be observed with a nanosecond apparatus. It is representative of the amount of events "one photon crosses the bulk of one particle". The consequence on the TOF is a delay $\Delta t = 60\ fs$ per event (case of large particles). For an optical thickness of 20, the global effect is roughly equal to 20*60 = 1.2 *ps.* The real simulation we have carried gives the same order of magnitude (2.54 *ps*). The impact of the global TOF is very small but as soon as it is measurable, it exhibits a neat sensitivity to the absorption coefficient of particles.

8. Conclusion

We have carried a detailed study of TOF of light going through a scattering media when the particles are absorbing. We have demonstrated that TOF is significantly reduced by the absorption process inside the particle for 3 main reasons. First, the absorption inside the bulk of the particle kills delayed Debye modes. Then, phase functions are more peaked in the forward direction. Finally, single scattering trajectories are enhanced compared to multiple ones due to the albedo of particles and the energy losses observed for every scattering event. We have focused on two particular regimes: small particles $R = 5\ \mu m$ and large particles $R = 50\ \mu m$. For small particles, TOF is reduced for value of k_{pa} ($\geq 10^{-3}$) only. For large particles, the effect can be tracked for value of k_{pa} ($\geq 10^{-5}$). Measurements of the time of flight, coupled with other techniques, could be a good way to measure the absorption coefficient of a particle with a good sensitivity.

#154880 - $15.00 USD Received 16 Sep 2011; revised 28 Oct 2011; accepted 28 Oct 2011; published 20 Dec 2011